Optiska neinvazīva hibrīdmetode agrīnai sepses diagnostikai un terapijas vadībai
ERAF Nr.1.1.1.1/16/A/065

08.03.2017. - 07.06.2018.

LU ASI, Rīga

Projekta darbības (aktivitātes)

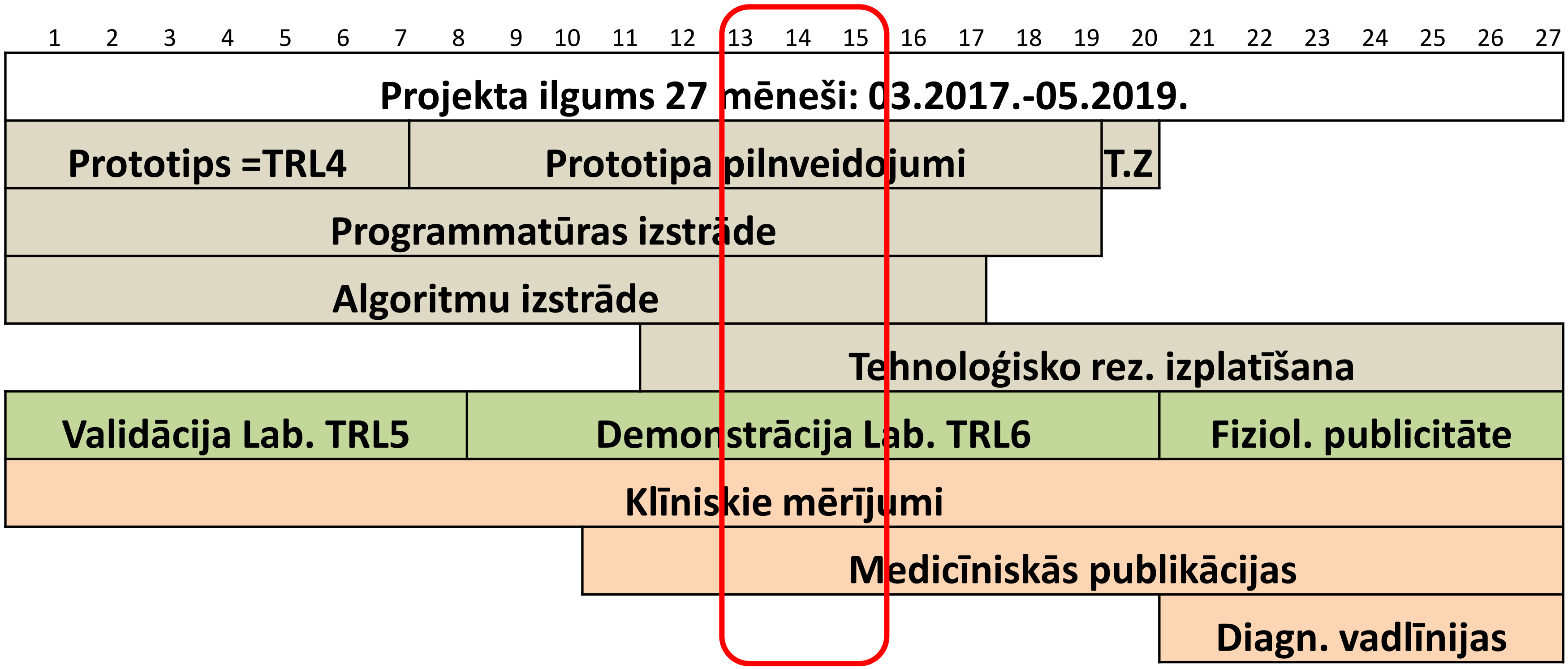

T.z. = tehnoloģiskā zinātība

Publicitāte

- Dalība zinātniskajās konferencēs SPIE Photonics Europe 2018 un ISICEM39 (Darbība 1.4., 3.3.)

Mutiskais ziņojums: Hyperspectral evaluation of skin blood oxygen saturation at baseline and during arterial occlusion, Z. Marcinkevičs, + SPIE Proc. **Open Access**

Postera ziņojums: Snapshot hyperspectral system for noninvasive skin blood oxygen saturation monitoring, U. Rubins, + SPIE Proc.

Postera ziņojums: Skin oxygenation, biomarkers of endothelial injury and their association with severity of illness in patients with septic shock, S. Kazune, + Critical Care Suppl. (IF 6.5)

Tehnoloģiju izstādes apmeklējums

Intelligent Hyperspectral Imaging Holds Promise for Pathology

Technological advancements enable fast and high-resolution hyperspectral imaging for the research and clinical markets.

BY HOD FINKELSTEIN, RON R. NISSIM AND MARK J. HSU, TRUTAG TECHNOLOGIES INC.

Hyperspectral imaging (HSI) provides images with numerous spectral bands over a continuous spectral range, enabling analysis of complex scenes that contain both spectral and spatial information. These imagers tend to be expensive and often require external processing of the large amounts of data captured in each scan. Recent advances in tunable filter elements combined with increased computational power of embedded processors have resulted in a fully autonomous battery-operated and small form-factor imager. The imager can capture a full hyperspectral data cube and distill it to the information of interest in less than five seconds and at a price point that previously had been unattainable.

Much of the spectral information in nature is broadband — the sun's blackbody emission spectrum, the reflectance spectrum of flowers and the absorption spectrum of blood are just a few examples. In order to minimize the amount of sensory information that needs to be processed by our brains, nature developed optical sensors in the form of cone-shaped cells in our retinas. These have broad absorption spectra in the blue, green and red regions of the spectrum.

Solid-state image sensors, such as the CCD and the CMOS sensor, are inherently monochromatic. They convert the photons that are absorbed within the depletion region of their PN junctions into charge, regardless of their wavelength. In order to mimic our color perception, broadband polymer color filters are deposited on top of these junctions to create a color filter array (CFA). Similarly to our cone cells, these filters transmit in the blue, green and red regions of the spectrum. Pixel arrays coated with such CFAs are commonly known as RGB sensors.

In reality, significant information can be gleaned from fine spectral features. These features may arise naturally or be custom designed. High-resolution spectral information in nature is used to identify atomic and molecular emission and absorption lines and subtle spectral shifts because of metabolic changes in tissue, as well as to recognize plants, animals or various pathologies.

In recent years, various man-made optical labels have been introduced and widely used to tag biological targets. These include fluorescent molecules and quantum dots, each having a characteristic spectrum. Observing these objects and processes with RGB sensors is akin to a farsighted person trying to read a book: The person may be able to read the chapter titles, but not their contents. Hyperspectral imagers address the need to collect optical information with both high spatial and spectral resolutions, thus enabling us to acquire a more accurate picture of biological objects and processes.

Spatial and spectral resolution

In order to understand how HSIs work, it is helpful to understand two related sensing technologies. Spectrometers analyze the spectral content of light without acquiring information in the spatial distribution of these spectra. As such, they work well for analyzing bulk homogenous materials. Such devices are quite simple and recently have been integrated into cellphones.

Figure 1. TruTag Model 4100 handheld hyperspectral imager collects optical information with high spatial and spectral resolutions.

Tehnoloģiju izstādes apmeklējums

Biofotonikas konferences apmeklējums

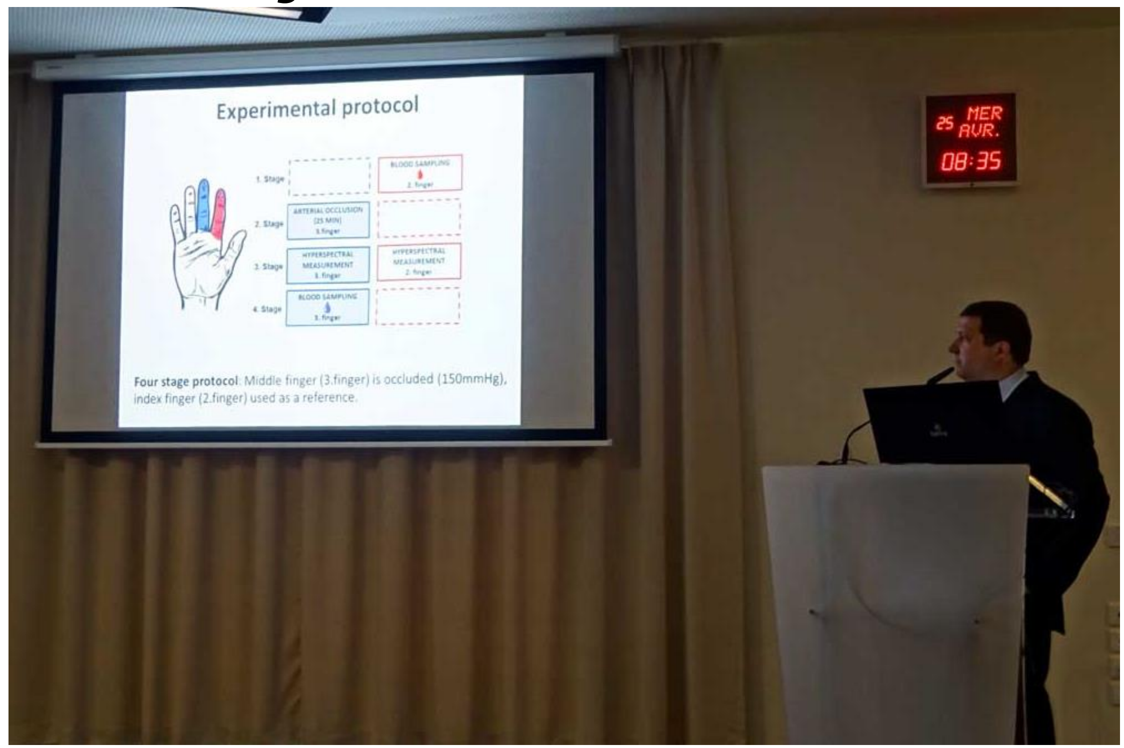

SPIE Photonics Europe 2018, Strasbūra, Francija, 22-26 aprīlis

Metodes validācija laboratorijas apstākļos (Darbība 2.2.)

ROI uz ceļgala pirms HSI reģistrācijas

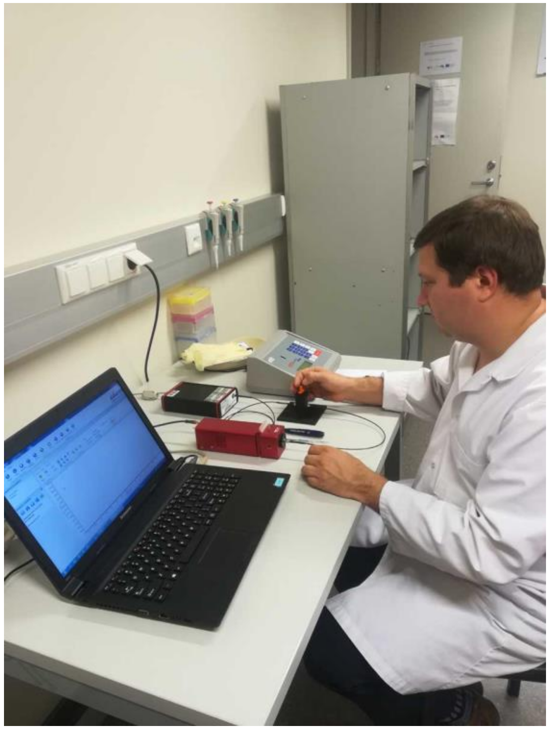

Asins parauga spektroskopija, skābekļa saturācijas noteikšana

- Asins paraugu spektroskopija (Darbība 1.2.)

Caurizgājušā starojuma spektroskopiskā analīze 520nm – 650 nm diapazonā

Bēra-Lamberta caurizgājušās gaismas transporta modeļa kalibrācija

SaO2 (%) Model	SaO2 (%) Data
6.29	8.5
13.1	16.3
46.4	45.4
66.0	74.1
68.9	75.5
81.3	90.9
90.6	95.4

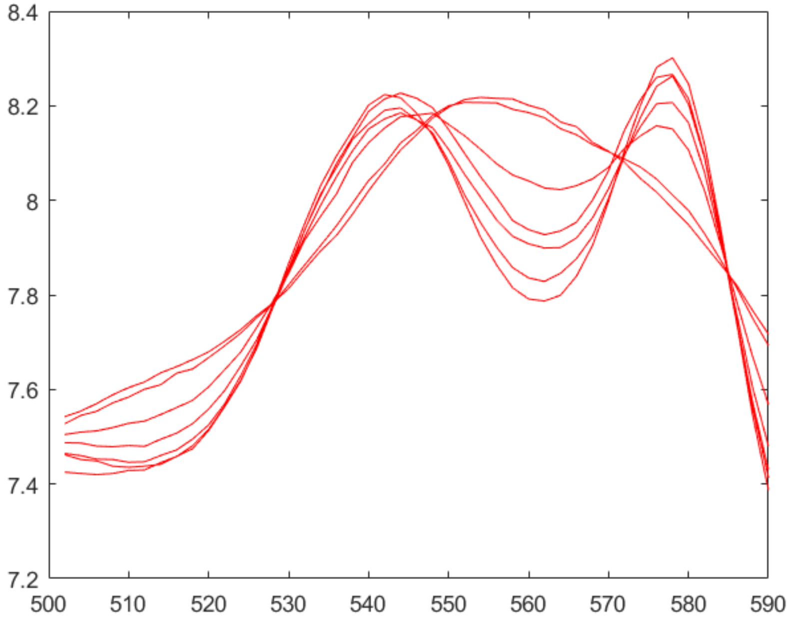

Asins paraugi miera apstākļos

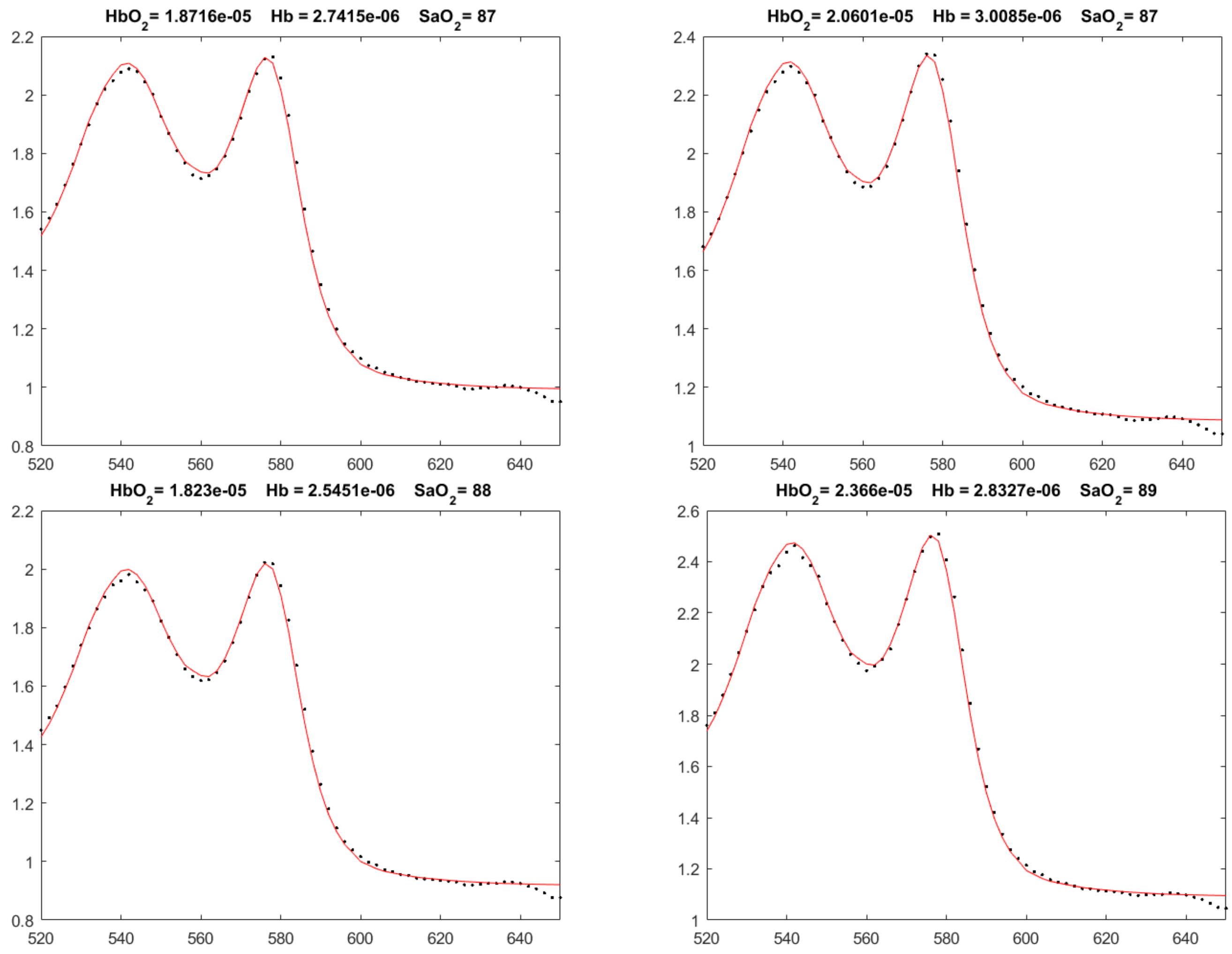

Asins paraugi oklūzijas laikā

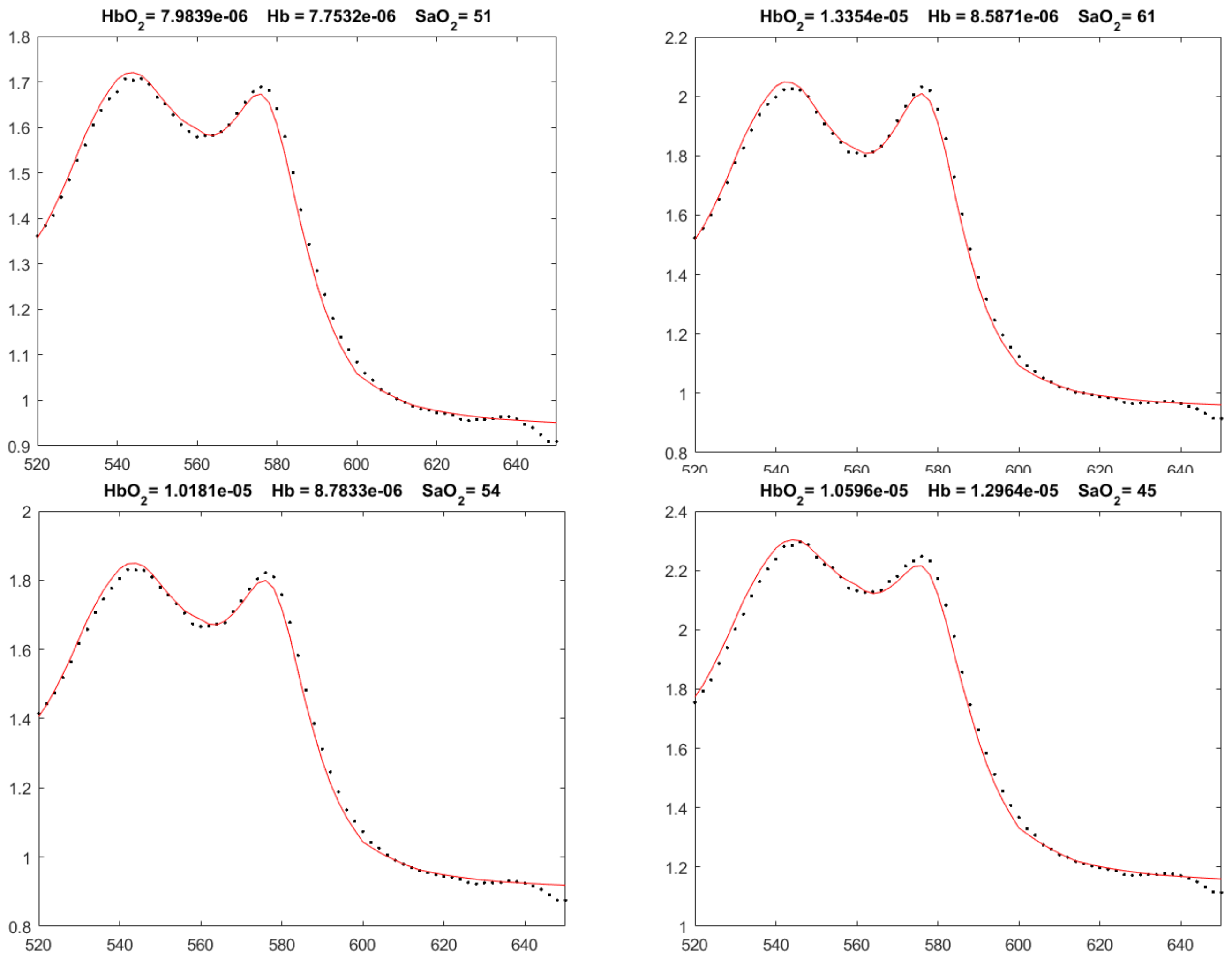

Asins paraugu spektroskopija

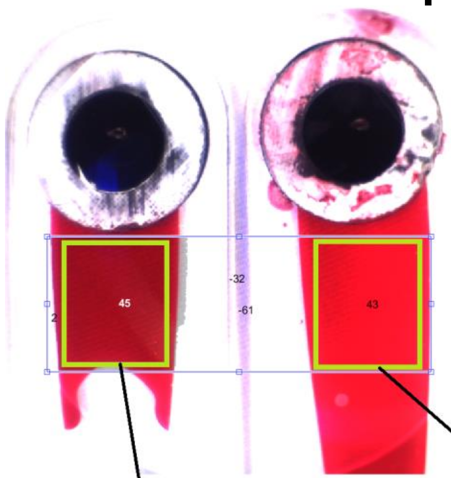

Zaļajā spektra diapazonā (500-600nm) asinīm ir pārāk liela absorbcija, un modelis nespēj izšķirt spektrā oksi-hemoglobīna maksimumus, aprēķina kļūdainas SaO2 vērtības.

Problēmas novēršanai, Nuance kamerai nepieciešams papildus zaļais gaismas avots

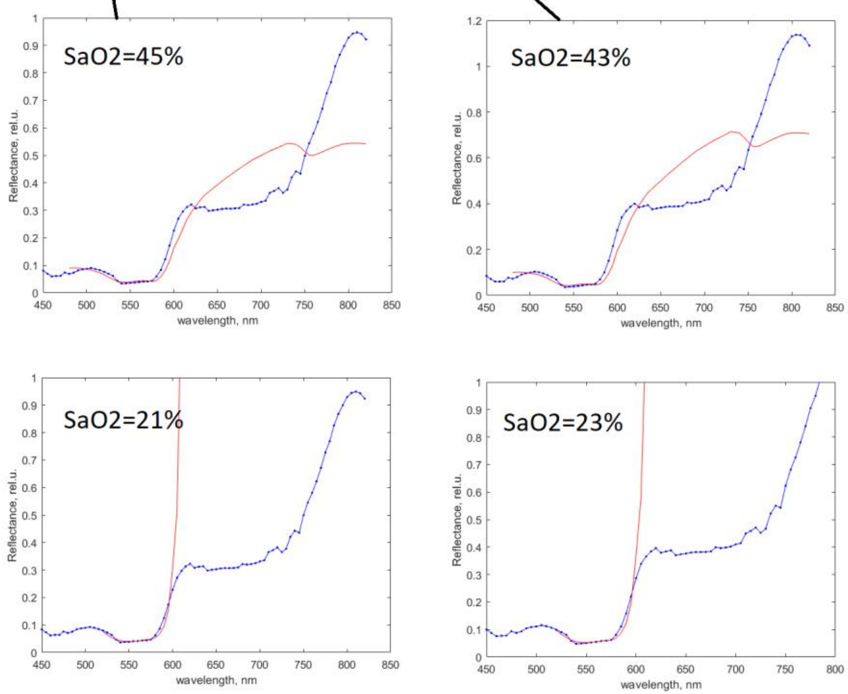

480-820nm

520-610nm

Hiperspektrālās kameras kalibrācija

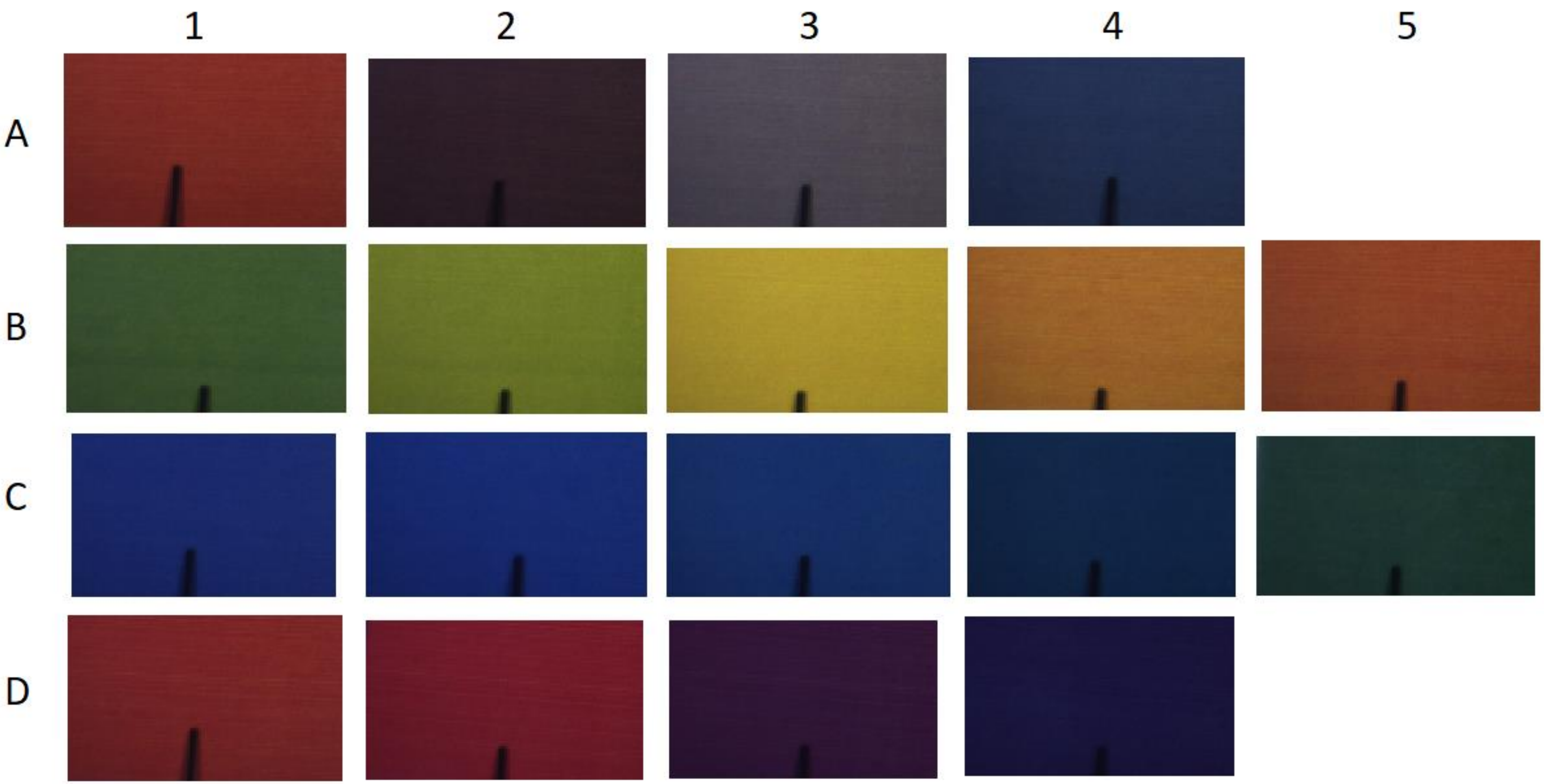

Nuance un spektrometra spektru salīdzinājums

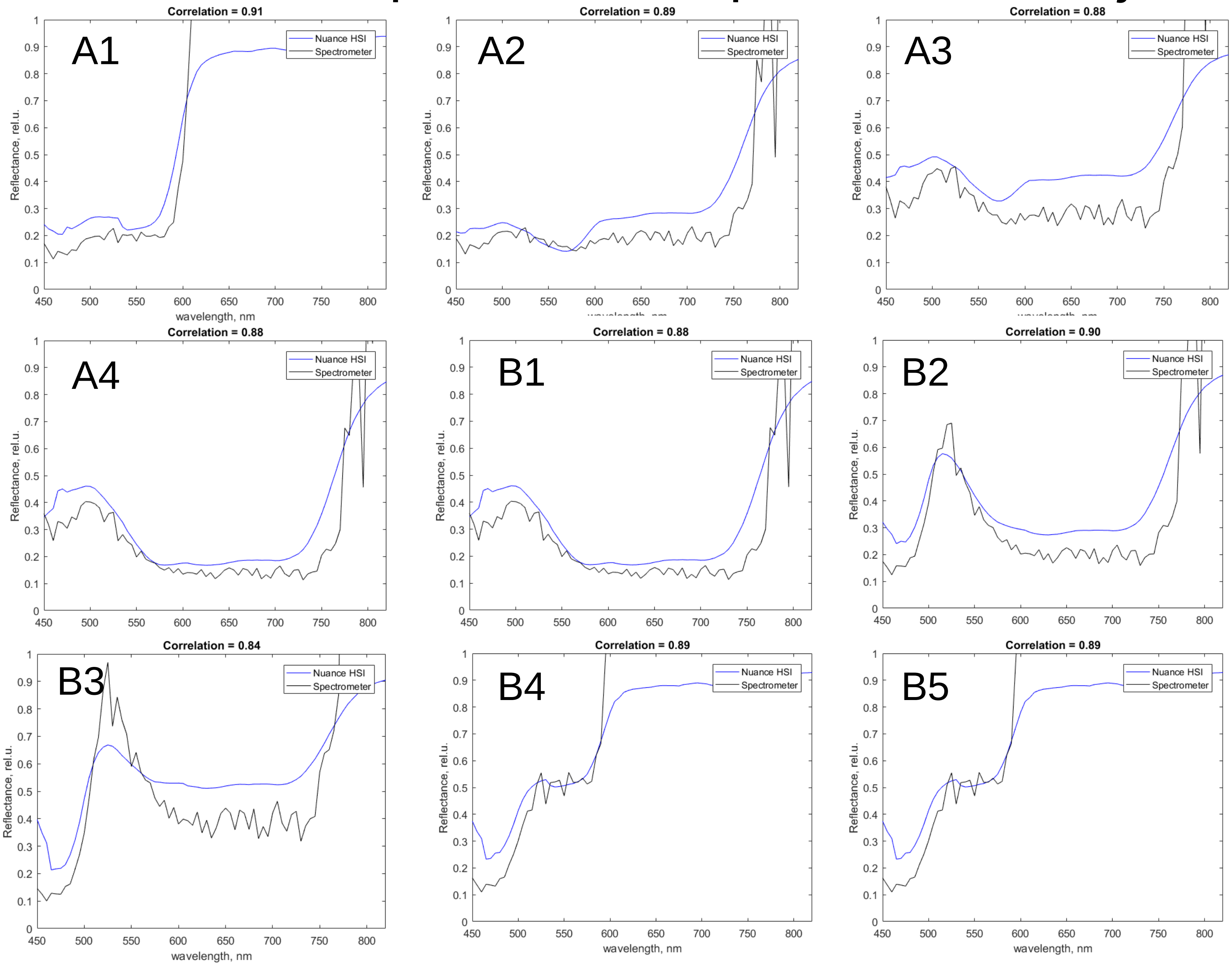

Nuance un spektrometra spektru salīdzinājums

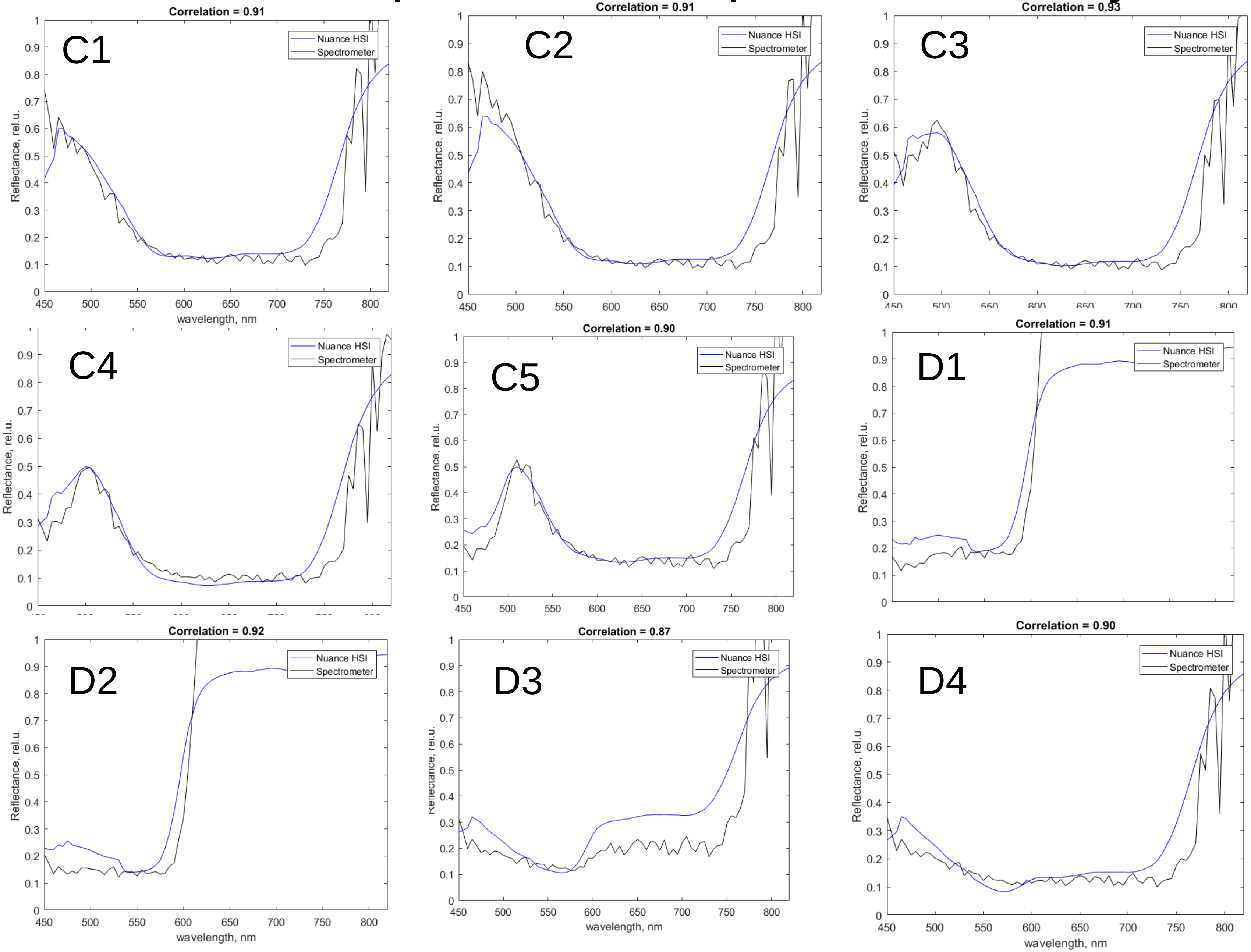

- Gaismas difūzā transporta modeļa izveide (Darbība 1.3.)

Projektā iesaistījusies Mg. Phys. I. Ošiņa. Darba uzdevumi: difūzijas matemātiskā modeļa pilnveidojumi, asins skābekļa saturācijas noteikšanai no hiperspektrālo attēlu datiem.

Difūzijas teorija

Enerģijas saglabāšanās

Neņem vērā:
- polarizāciju
- koherenci
- nelinearitāti
- neelastīgu izkliedi

iegūtā enerģija izkliedes dēļ dE_{sca}

starojums

zaudētā enerģija absorbcijas dēļ dE_{ext}

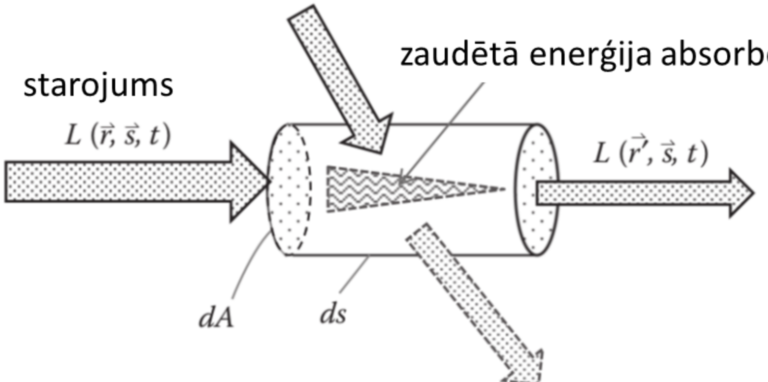

zaudētā enerģija izkliedes dēļ dE_{div}

$dV = dAds$

\+ enerģija, kas tiek ģenerēta sistēmā no starojuma avotiem dE_{sou}

- $dE = -dE_{div} - dE_{ext} + dE_{sca} + dE_{sou}$
- $dE = \frac{\partial L(\vec{r},\vec{s},t)}{c\partial t} dV d\omega$

Bolcmaņa vienādojums

$$\frac{1}{c}\frac{\partial L(\vec{r},\vec{s},t)}{\partial t} = \underbrace{-\nabla \cdot \partial L(\vec{r},\vec{s},t)}_{dE_{div}} \underbrace{- \mu_t \partial L(\vec{r},\vec{s},t)}_{dE_{ext}} + \underbrace{\mu_s \int_{4\pi} \partial L(\vec{r},\vec{s},t) p\left(\vec{s'} \cdot \vec{s}\right) d\omega'}_{dE_{sca}} + \underbrace{S(\vec{r},\vec{s},t)}_{dE_{sou}}$$

Difūzijas tuvinājums

- $\mu_s \gg \mu_a$
- Izkliedējošās un absorbējošās vielas ir izvietotas vienmērīgi
- Difūzais starojums izplatās pēc Fika likuma (no vietas ar lielāku koncentrāciju uz vietu ar mazāku koncentrāciju)

$$\vec{\boldsymbol{j}} = -\boldsymbol{\zeta}\vec{\boldsymbol{\nabla}}\boldsymbol{\varphi}$$

$$\zeta = \frac{1}{3(\mu_a + \mu_s')} \qquad \mu_s' = (1-g)\mu_s$$

- Stacionārais difūzijas vienādojums

$$\vec{\boldsymbol{\nabla}} \cdot \vec{\boldsymbol{j}} = -\boldsymbol{\mu_a}\boldsymbol{\varphi} + \boldsymbol{q} \qquad q = \mu_s I(z)$$

- Bēra-Lamberta likums

$$\boldsymbol{I}(\boldsymbol{z}) = \boldsymbol{I_0}\boldsymbol{exp}(-\boldsymbol{\mu}\boldsymbol{z}) \qquad \mu = \mu_a + \mu_s$$

ζ – difūzijas konstante
φ – starojuma intensitāte
$\vec{j}$ – vidējā fotonu plūsma
μ_a – absorbcijas koeficients
μ_s' – reducētais izkliedes koeficients
μ_s – izkliedes koeficients
g – anizotropijas faktors $< cos\theta >$
q – avota funkcija – difūzais starojums, kas radies no krītošās gaismas

Starojuma intensitāte

$$\vec{j} = -\zeta\vec{\nabla}\varphi$$
$$\vec{\nabla}\cdot\vec{j} = -\mu_a\varphi + q$$

$$\boldsymbol{\vec{\nabla}^2\varphi - \frac{\varphi}{\delta^2} = -\frac{q}{\zeta}}$$

- Ja intensitāte ir atkarīga tikai no dziļuma:

$$\frac{d^2\varphi(z)}{d^2z} - \frac{\varphi(z)}{\delta^2} = -\frac{q(z)}{\zeta}$$

atrisinājums

$$\boldsymbol{\varphi = \frac{I_0\delta^2\mu_s}{\zeta(1-\mu^2\delta^2)}\exp(-\mu z) + A_1\exp\left(-\frac{z}{\delta}\right) + A_2\exp\left(\frac{z}{\delta}\right)}$$

$$\zeta = \frac{1}{3\mu_s} \qquad \delta = \frac{1}{\sqrt{3\mu_s\mu_a}}$$

δ – optiskais iespiešanās dziļums
I_0 – starojuma intensitāte uz virsmas
A_1, A_2 – brīvie koeficienti, kas jānosaka no robežnosacījumiem

Robežnosacījumi

$$E = \frac{\varphi}{4} \pm \frac{j}{2}$$

fotonu enerģijas plūsma uz laukuma vienību
+ ir z pieaugšanas virzienā (dziļumā), **-** ir z samazināšanās virzienā (uz ādas virskārtu)

$$j = -\zeta \frac{d\varphi}{dz}$$

fotonu plūsma
no šī nosaka φ

$$R_{12}\left(\frac{\varphi}{4} + \frac{j}{2}\right)\Big|_{z=d-0} + (1 - R_{21})\left(\frac{\varphi}{4} - \frac{j}{2}\right)\Big|_{z=d+0} = \left(\frac{\varphi}{4} - \frac{j}{2}\right)\Big|_{z=d-0}$$

$$(1 - R_{12})\left(\frac{\varphi}{4} + \frac{j}{2}\right)\Big|_{z=d-0} + R_{21}\left(\frac{\varphi}{4} - \frac{j}{2}\right)\Big|_{z=d+0} = \left(\frac{\varphi}{4} + \frac{j}{2}\right)\Big|_{z=d+0}$$

R_{12}, R_{21} – efektīvie atstarošanās koeficienti atbilstoši apgabalā $d - 0$ un $d + 0$

$$j\Big|_{z=d+0} = j\Big|_{z=d-0} = j$$

uz robežvirsmas ar gaisu

$$\varphi\Big|_{z=+0} = -2\,\frac{1+R}{1-R}\,j\Big|_{z=+0}$$

3 slāņu gadījumā

$$\begin{cases} j_1(0) = -A\varphi_1(0) \\ \varphi_1(d_1) = \varphi_2(d_2) \\ j_1(d_1) = j_2(d_2) \\ \varphi_2(d_2) = \varphi_3(d_3) \\ j_2(d_2) = j_3(d_3) \end{cases}$$

$$\gamma = \frac{-j|_{z=+0}}{I_0}$$

Atstarošanas koeficients

Absorbcijas un izkliedes koeficienti

$$\mu_s(\lambda) = \mu_s'(\lambda_r)\left(\frac{\lambda}{\lambda_r}\right)^{-\gamma}$$ absorbcijas koeficients

Saistīts ar Releja izkliedi

Saistīts ar Mī izkliedi

$$\mu_s(\lambda) = \mu_s'(\lambda_r)\left[\rho\left(\frac{\lambda}{\lambda_r}\right)^{-4} + (1-\rho)\left(\frac{\lambda}{\lambda_r}\right)^{-\gamma}\right]$$ izliedes koeficients

Hiperspektrālo attēlu apstrādes programma (2 slāņi)

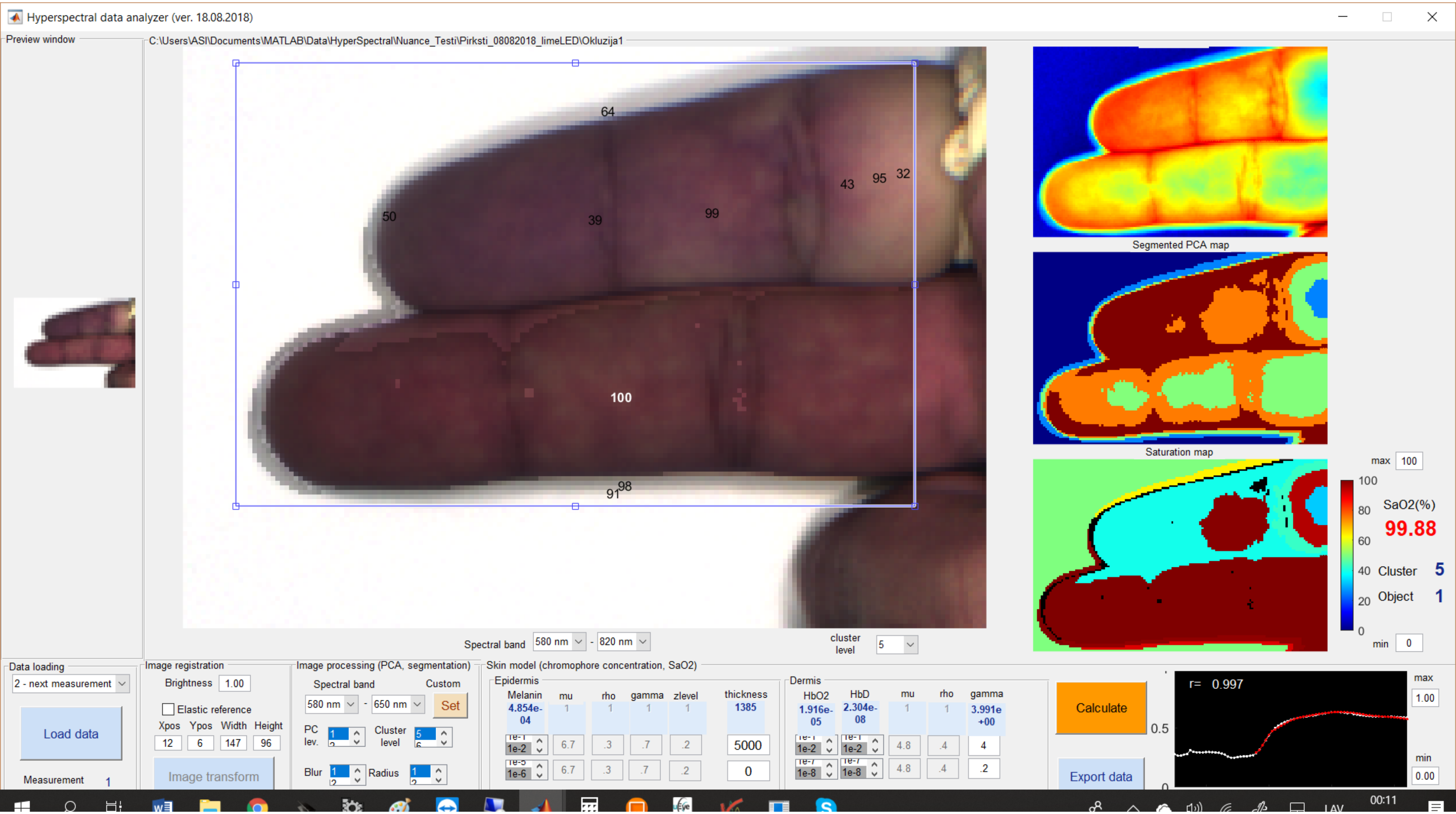

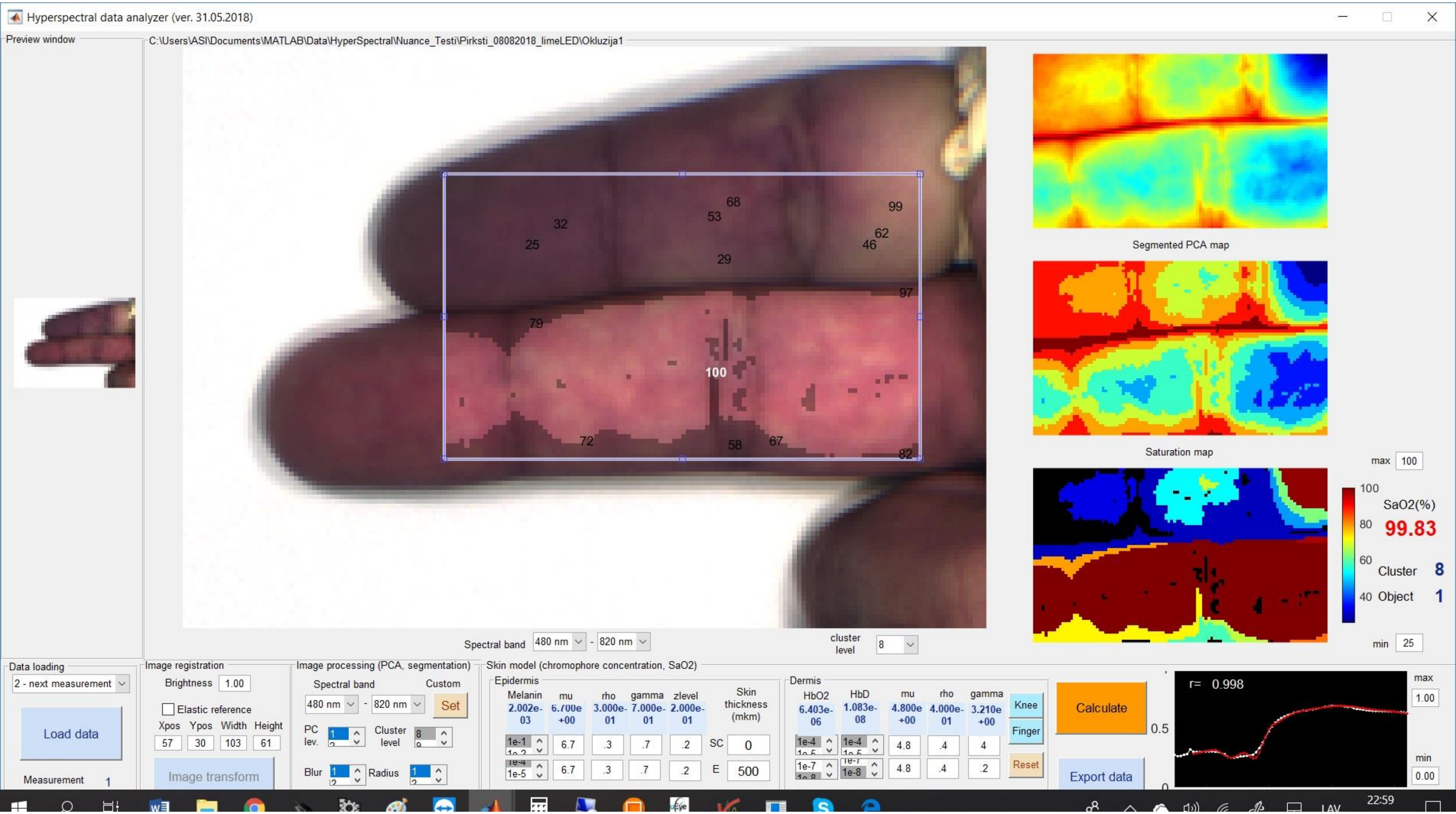
Hyperspectral data analyzer (ver. 31.05.2018)
Preview window
C:\Users\ASI\Documents\MATLAB\Data\HyperSpectral\Nuance_Testi\Pirksti_08082018_limeLED\Okluzija1
Segmented PCA map
Saturation map
max 100
SaO2(%)
99.83
Cluster 8
Object 1
min 25
Spectral band 480 nm - 820 nm
cluster level 8
Data loading
2 - next measurement
Load data
Measurement 1
Image registration
Brightness 1.00
Elastic reference
Xpos Ypos Width Height
57 30 103 61
Image transform
Image processing (PCA, segmentation)
Spectral band Custom
480 nm - 820 nm Set
PC lev.
Cluster level
Blur
Radius
Skin model (chromophore concentration, SaO2)
Epidermis
Melanin mu rho gamma zlevel
Skin thickness (mkm)
SC 0
E 500
Dermis
HbO2 HbD mu rho gamma
Knee
Finger
Reset
Calculate
Export data
r= 0.998
max 1.00
min 0.00

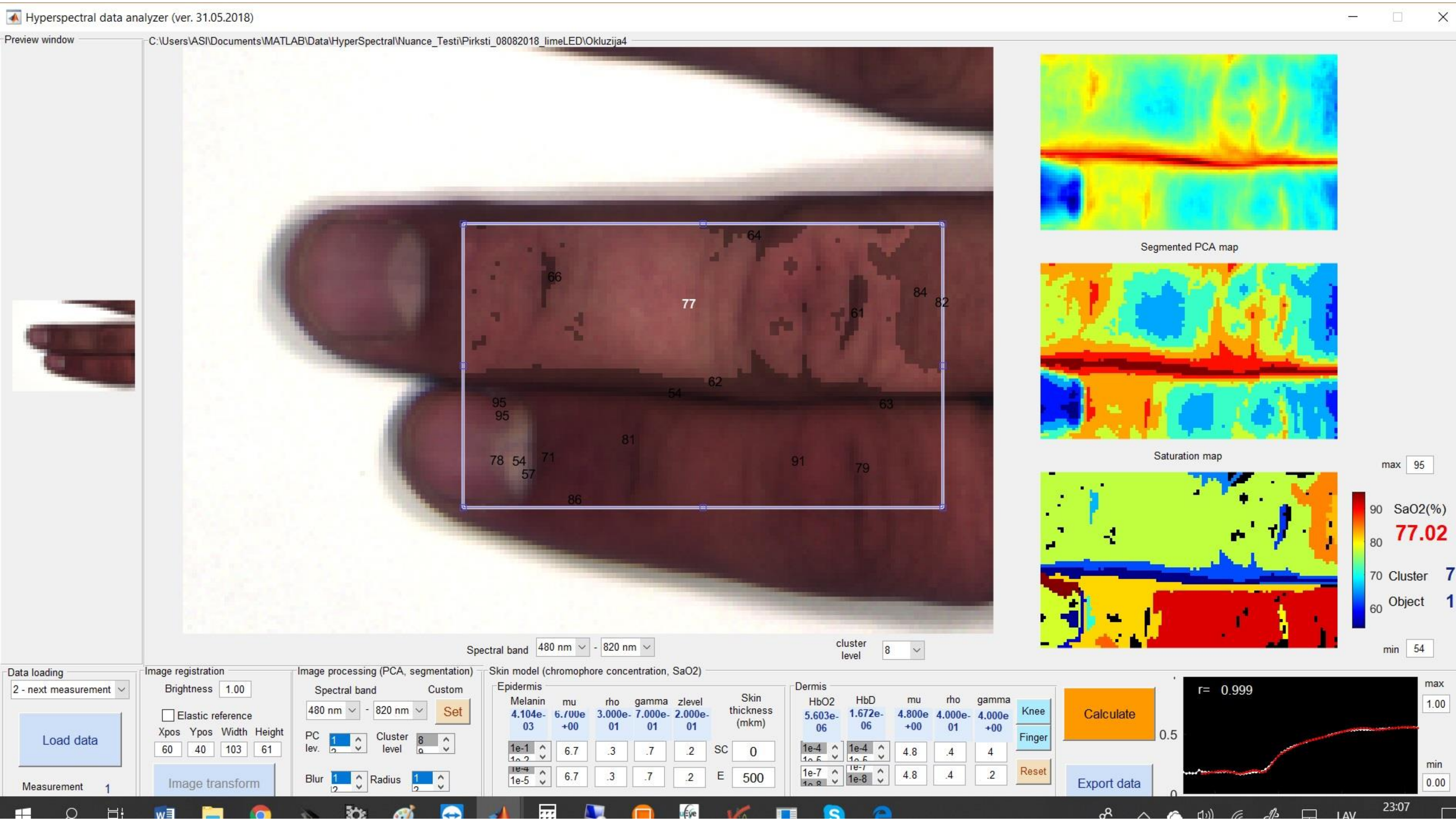
Hyperspectral data analyzer (ver. 31.05.2018)
Preview window
C:\Users\ASI\Documents\MATLAB\Data\HyperSpectral\Nuance_Testi\Pirksti_08082018_limeLED\Okluzija4
Segmented PCA map
Saturation map
max 95
min 54
SaO2(%)
77.02
Cluster 7
Object 1
Spectral band 480 nm - 820 nm
cluster level 8
Data loading
2 - next measurement
Load data
Measurement 1
Image registration
Brightness 1.00
Elastic reference
Xpos Ypos Width Height
60 40 103 61
Image transform
Image processing (PCA, segmentation)
Spectral band
Custom
Set
PC lev.
Cluster level
Blur
Radius
Skin model (chromophore concentration, SaO2)
Epidermis
Melanin 4.104e-03
mu 6.700e+00
rho 3.000e-01
gamma 7.000e-01
zlevel 2.000e-01
Skin thickness (mkm)
SC 0
E 500
Dermis
HbO2 5.603e-06
HbD 1.672e-06
mu 4.800e+00
rho 4.000e-01
gamma 4.000e+00
Knee
Finger
Reset
Calculate
Export data
r= 0.999
max 1.00
min 0.00